

Chapter 1

Principles of Atomic Force Microscopy



Wanxin Sun

Abstract Clearly understanding the working principles of different modes of atomic force microscopy (AFM) is important for users to choose suitable measurement modes for their research projects, optimize working parameters, identify artifacts, and interpret data. In this chapter, conventional imaging modes and force modes will be discussed first, followed by the introduction of recent developments in AFM quantitative nano-mechanical properties measurement.

Since it was invented three decades ago (Binnig G, Quate CF, Gerber C, *Phys Rev Lett* 56:930–933, 1986), AFM has been becoming a more and more important instrument in nano science and technology. The uniqueness of AFM is its capability of providing nanometer spatial resolution in three dimensions while no vacuum or contrast reagent is needed. AFM has been extensively used in virtually every branch of science and engineering and contributes to many discoveries in nanomaterials, such as the discovery of graphene. In recent years, AFM has been further developed in three aspects. 1. conveying more material related information, such as mechanical, electrical, magnetic and thermal properties at nanometer scale; 2. integrating with different advanced optical techniques, including Raman, fluorescence, infrared spectroscopy; 3. incorporating with environment control for life science and material researches, such as temperature, liquid environment with pH and other ion strength control, light illumination. With these developments, AFM has been extending its applications beyond topographic imaging, such as polymer phase transition under different temperature, I-V characteristics in today's semiconductor devices, live cell dynamics under different chemical/mechanical stimuli, molecular dynamics under different temperature and chemical environments.

On the other hand, the expanded capabilities of AFM make it difficult for users to choose a proper measurement mode, suitable probes and optimize operation parameters. Many efforts have been made to develop different smart scan modes, including peak force tapping developed by Bruker, where software can tune operation parameters to achieve optimized image quality. However, it is still users' task

W. Sun (✉)
Bruker Nano Surface, Singapore, Singapore
e-mail: wanxin.sun@bruker.com

to choose measurement modes, identify artifacts, interpret data for their research projects. All these need users to clearly understand the working principles of different modes. In this chapter, conventional imaging modes and force modes will be discussed first, followed by the introduction of recent developments in AFM quantitative nano-mechanical properties measurement.

1 AFM Working Principles

In AFM, a sharp probe runs a raster scan across the sample surface with a positioning accuracy in sub-nanometer level. During the scan, the probe is moved up and down by a feedback close loop to maintain a constant probe-sample interaction. The vertical movements are recorded against XY position to form a surface topography of the sample, as shown in Fig. 1.1. The nano positioning in an AFM is achieved by

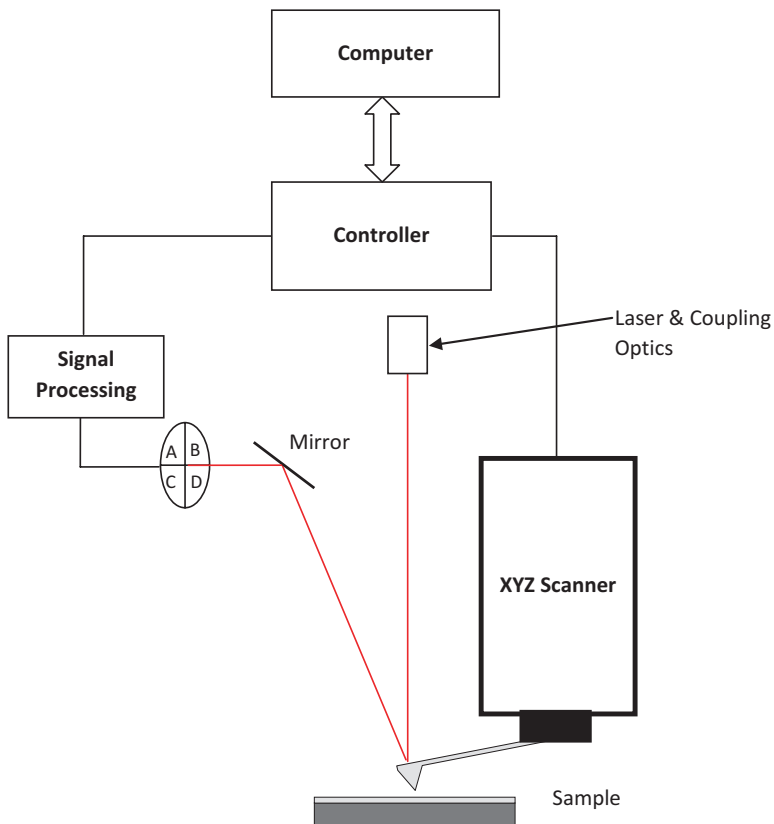
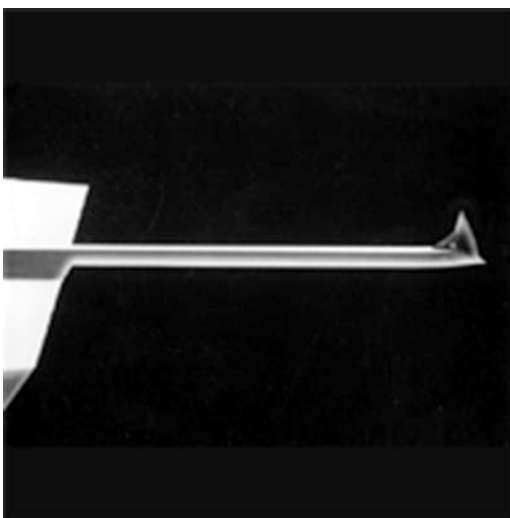


Fig. 1.1 Schematic diagram of an atomic force microscope. (The diagram is not in scale.) The laser emitted from the laser diode is focused onto the end of the cantilever. The reflected laser beam is redirected to a quadrant photodiode. The vertical and lateral movements of the cantilever is detected by the photodiode. The feedback close loop is implemented in the controller. The computer is used to setup parameters for the controller and collect data from it to form images

piezoelectric scanners, where the movements in XYZ are driven by high voltages in the range of hundreds of volts. Intrinsically, piezoelectric material does not response linearly to the voltage applied. If linear voltages are applied to the scanner, the recorded images are distorted by the nonlinear motion of piezo scanner. To correct this issue, there are two prevailing methods in today's AFMs. One is to add XYZ position sensors to monitor actual movements of the scanner and correct the nonlinearity through a feedback close loop, where the voltages applied to the scanner are tuned until the scanner reaches the desired positions. This method is usually called close loop. Different position sensors have been developed for AFM, including capacitive sensor, inductive sensor, strain gauge, and optical sensors. All of them work well as long as they are implemented properly. The other approach is to model the nonlinearity first, and then use nonlinear voltage to drive the scanner to obtain linear movement. In this approach, a certified calibration grid is scanned by the scanner with different scan speed, scan size, scan angle etc. After a series of images are collected, the parameters in the model of scanner movement against applied voltage and scan conditions are extracted by fitting all the images. This method is usually called open loop. Traditionally, open loop is used for high resolution scan as it does suffer from the added noise from the position sensors. With the advances in sensor developments, close loop in today's AFM can achieve similar high resolution performance to open loop. Therefore, more and more users use close loop for routine sample measurement and open loop for atomic resolution measurement.

The commonly used AFM probes consist of a sharp tip and a micro cantilever, as shown in Fig. 1.2. The radius of curve of the today's AFM tip ranges from a few nm to 30 nm, depending on fabrication process and their applications. The micro cantilever is 30–40 μm in width and 125–450 μm in length. The thickness ranges from a fraction of μm to a few μm .

Fig. 1.2 Scanning electron microscopic image of a typical AFM probe, consisting of a sharp tip and a micro cantilever



The cantilever works as a sensor to detect the probe-sample interaction. The interaction between the probe and sample surface is complicating and many types of forces are involved [2]. The detailed discussion about the origins of the interaction forces is beyond the scope of this chapter. Only the aspects directly related to AFM instrumentation and applications, for example, the magnitude of the overall interaction forces, cantilever dynamics changes due to force gradient or energy dissipation during probe-sample interaction, will be discussed. The normal force between the probe and the sample is measured by the cantilever bending, which simply follows Hook's law,

$$F = k\Delta z \quad (1.1)$$

where k is the spring constant of the cantilever, Δz is the cantilever bending in nm.

With a variety of cantilevers available commercially, AFM can measure forces ranging from a few pN to hundreds of μN .

To measure the tiny bending or twisting of cantilever, an optical lever detection scheme is well adopted in AFM, as shown in Fig. 1.3. The laser beam from a laser diode is focused onto the end of the cantilever. The reflected beam from the cantilever surface is redirected to a quadrant photodiode, which is usually called position sensitive photodiode (PSPD) in AFM. When the cantilever bends vertically, the direction of the reflected laser beam changes accordingly. Then the laser spot on the PSPD shifts vertically. In the same way, the twist of the cantilever will cause laser spot on PSPD move laterally. The position of the laser spot is measured by the output of PSPD, i.e. $((A + B) - (C + D)) / (A + B + C + D)$ is proportional to vertical position. $((A + C) - (B + D)) / (A + B + C + D)$ is proportional to lateral position. The

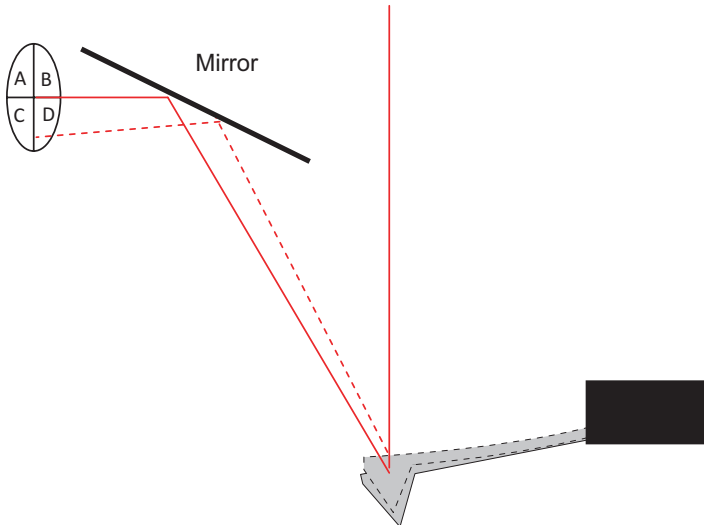


Fig. 1.3 Schematic diagram of optical lever detection system. The solid line drawing and dashed line drawing are laser beams for two cantilever deflection states

normalization to the sum signal of $(A + B + C + D)$ is to eliminate the effect of cantilever reflectivity. It is noted that the optical lever measures the angle of cantilever deflection, not the displacement. Therefore, short cantilever is more sensitive to detect deflection changes.

2 Contact Mode

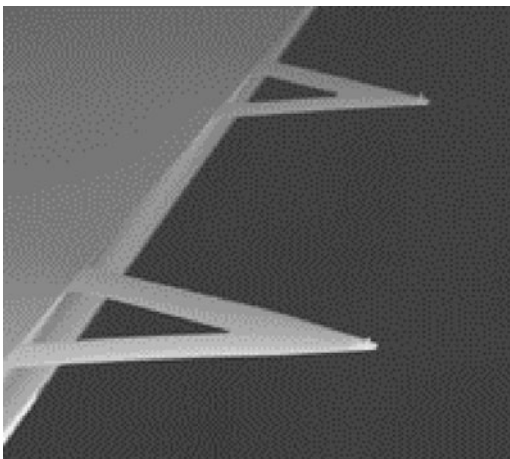
In contact mode, the normal force, i.e. the vertical deflection of cantilever, is maintained at a constant during scan. When the probe scans across a protruding feature, the cantilever is pushed up, generating an error in vertical deflection. To eliminate this error, the controller will lift the probe until the error becomes zero. For a recessed feature, the probe is lowered to eliminate the deflection error. With an optimized feedback loop, the probe tracks the surface with a constant force to form the topography of the sample. During the scan, lateral/frictional force always exists between the probe and sample. Lateral force can form an image mapping the lateral/friction force distribution across the sample surface, which is called lateral force microscopy (LFM). This has been used to study self-assembled monolayer [3], where different function groups show different frictional forces while their heights are almost the same. While providing rich information about local friction, lateral force also causes problems, for example, lateral force, if not controlled properly, can cause damage to delicate samples and wear out the sharp tip. Take live cells as an example, the measured Young's modulus is in the magnitude of kPa. Force higher than a few nN will cause significant deformation, which leads to low resolution, damage of features and molecules on the cell membrane, and inaccurate morphology. In addition, the force exerted by probe can also work as mechanical stimuli, which may induce a series of responses of cells, including cytoskeleton, focal adhesion complex etc. For biomolecules, large force may induce conformation changes. For live cells, the force should be control from sub nN to several nN. For biomolecules, the force should be ideally controlled to lower than 100pN.

To achieve sub nN force control, cantilever spring constant is a critical parameter. Softer cantilever deflects more under the same load, which is favorable for force detection sensitivity. However, the thermal noise of cantilever and environmental interference prevent users from using cantilevers with ultralow spring constant. For example, cantilevers with a lower spring constant suffer more thermal drift with the temperature variation. The heat generated by the AFM laser or microscope illumination often causes significant drift in deflection for cantilevers with spring constant lower than 0.01 N/m, in the range of a few volts in the PSPD output. Besides temperature, protein adsorption on the cantilever generates stress on one side, resulting in observable deflection change, which has been used as a sensor for protein detection [4]. The drift in cantilever deflection causes instability in imaging. For example, if the cantilever deflection increases with time, the probe will be lifted from the sample surface gradually. This is because the increase in cantilever deflection means higher repulsive force to the controller although it is caused by cantilever deflection

drift only. The response of the controller is to lift the cantilever. The probe may not track the surface anymore if the lift is significant, resulting in part of the image not bearing any sample information. To overcome this issue, higher force must be set to compensate the cantilever drift. Then the image is not obtained at a constant force. Higher force in some part of the image will cause the deleterious effects discussed above. Therefore, too stiff or too soft cantilever is not advisable for live cell imaging. In practice, cantilevers with a spring constant between 0.01 N/m and 0.1 N/m are usually good for imaging live cells. This kind of cantilever is made of silicon nitride in V shape, as shown in Fig. 1.4. Silicon nitride is less reflective than silicon. To increase its reflectivity, a thin layer of Au or Pt is coated on the backside of the cantilever. The thermal expansion coefficient of metal is different from that of silicon nitride, making cantilever bend with temperature change. To relieve the thermal drift, Bruker released a probe with Au coating only at the end of cantilever for laser reflection, the rest of cantilever is uncoated. This probe is insensitive to temperature change and good for cell imaging and force measurement.

AFM can image cells under pseudo physiological conditions with temperature and chemical environment control. To image with AFM, cells must be attached to a support surface. 50–70% confluence is a good trial for most cell types. Too low concentration will make it difficult to locate a cell for AFM imaging. Too high concentration sometimes causes cells overlapping with each other or loosely attached. A large number of cell types can adhere directly onto glass cover slip and plastic ware, e.g. petridish, by normal cell culturing. Whenever needed, Bunsen burner flame treatment [5] and adhesives [6, 7] can be used to enhance cell adhesion. The commonly used adhesives include polylysine, collagen, laminin, Cell-Tak, and PEG derivatives. To avoid debris or unattached cells sticking to the cantilever during imaging, it is advisable to rinse the cell preparation with filtered medium or buffer to remove the cell debris and unattached cells. To maintain the viability of cells, today's biological AFM is equipped with temperature control, CO₂ atmosphere control, gas purging, and perfusion apparatus.

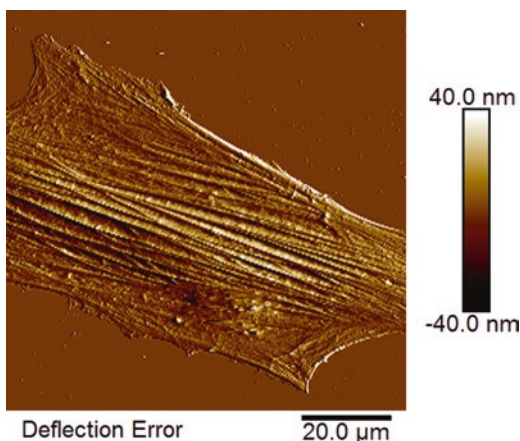
Fig. 1.4 Scanning electron microscopic image of a typical silicon nitride probe suitable for liquid imaging. This kind of probe usually has several cantilevers with different spring constants



As discussed previously, contact force is critically important for live cell imaging. Force adjustment is achieved by changing a parameter called deflection setpoint, at which the cantilever deflection is maintained during scan by the feedback loop. Larger setpoint means higher force. A force between 200pN and 500pN is a good starting point to try for contact mode imaging. A scan rate of 0.5–1 Hz is usually used for cell imaging. In AFM software, the line profiles in both directions (trace and retrace) are displayed. By adjusting the feedback loop gains and scan speed, the trace and retrace profiles will overlap with each other. Higher feedback loop gains make the probe tracking surface faster. On the other hand, oscillation will happen if the gains are set too high. In real operation, increase the gains until slight oscillation is observed. Then decrease the gains slightly to eliminate the oscillation. The highest gains without oscillation are the gains desired. With light force, AFM can produce the fine details on cell surface and accurate height of the cell. Accurate cell height is important to measure cell volume change of neurons during apoptosis. With large force, large deformation on the cell membrane is induced by the probe. The probe can “feel” the hard cytoskeleton filaments, the deflection error image provides rich information on cytoskeleton, as shown in Fig. 1.5. Researchers sometimes increase the force intentionally to get better contrast in cytoskeleton images.

In most time, the cantilever deflection baseline (deflection before the probe touches sample surface) is not zero due to thermal drift or laser adjustment. We need to consider the baseline when we set the setpoint. For example, if the deflection baseline is 200pN, and we want to use 300pN force to image, then setpoint will be 500pN. Therefore, deflection baseline must be measured before imaging. Force-distance curve is well accepted to determine the baseline. It will be discussed in details in the force measurement section. Here we just briefly introduce how to use force-distance curve to determine deflection baseline. After the cantilever is engaged onto the sample surface, the XY scan is stopped and the cantilever is ramped up and down at a specific point by the Z scanner. The cantilever deflection, which is proportional to the force, is recorded against the Z position of the cantilever. The typical

Fig. 1.5 Cytoskeleton revealed by deflection error in contact mode



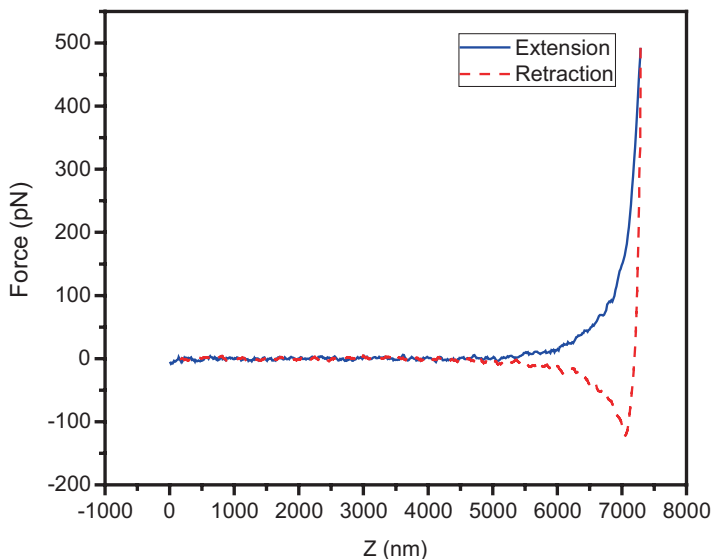


Fig. 1.6 Force-distance curve measured on a live cell. The solid line records the cantilever bending with the probe approaching the cell. The dashed line records the cantilever bending with the probe retracting from the cell. The retraction curve shows an adhesion force of about 150pN

force-distance curve on live cell is shown in Fig. 1.6. The flat region on the left is the cantilever deflection when the probe is not in touch with sample. The average of the flat region will be used as deflection baseline. After the force-distance curve is measured and a proper setpoint is set, the AFM is switched back to imaging mode.

3 Tapping Mode

Tapping mode is also known as intermittent contact mode or AC mode, where the cantilever is oscillated at its resonance frequency or slightly lower frequency. The oscillation is usually driven by a small piece of piezoelectric material embedded in the probe holder. The cantilever oscillation is measured by the changes in laser position on PSPD. The resonance frequency is found by sweeping drive frequency and finding the maximum oscillation amplitude. When the probe is brought to the sample surface by the engaging mechanism, the interaction between tip and sample causes decrease in oscillation amplitude and time lag between the drive signal and cantilever oscillation. At the bottom-most point of each oscillation cycle, the tip contacts the surface instantaneously. That is why tapping mode is also called intermittent contact mode. The amplitude decreases further when the probe is brought closer to the surface, and vice-versa. Thus, the amplitude is a direct measure of tip-sample interaction and the probe is moved up/down during XY raster scan to maintain constant amplitude. The up/down movements against XY position are recorded to form

topography. The time lag is measured by the phase difference between drive signal and cantilever oscillation. Both the amplitude and the phase lag are measured by a lock-in amplifier in AFM. Phase lag is caused by the energy dissipation during each oscillation cycle of the cantilever. When the probe contacts the sample surface, the sample surface undergoes both elastic and plastic deformation, causing energy lost. When it retracts from the sample surface, it often needs to overcome the attractive force and adhesive force. The adhesive force is also a cause for energy lost. Phase lag is related to viscoelastic properties of the sample. Phase lag mapping, also called phase imaging, has been extensively used to differentiate different materials [8].

In practical AFM operation, the operation amplitude (amplitude setpoint) is chosen at about 80% of the free cantilever amplitude. The origin of the phase shift is the resonance frequency shift under tip-sample interaction. How much the phase shifts depends on the material viscoelasticity and the operation parameters. Although phase image has been used extensively in differentiating different materials, such as phase separation in copolymer [9], there is ambiguity in material identification due to its intrinsic nature that phase shift is affected by operation parameters as well as material viscoelasticity. The contrast in phase image can be reversed under different operation conditions. Under light tapping, phase contrast is caused by the adhesive force sensed by the probe. With the increase in tapping force, the material deformation contributes more in the phase contrast. Therefore, the phase contrast under light tapping originates from the adhesiveness, which is often affected by relative humidity in ambient environment. In liquid environment, phase contrast under light tapping has been used to recognize molecules [10]. Under hard tapping, the phase contrast is the combination of adhesive force and material deformation.

Compared with contact mode, the probe contacts sample surface instantaneously in tapping mode. The lateral force is negligible. Tapping mode is good for loosely bound samples, which are easily pushed away by the probe in contact mode. In general, biomolecules and nanoparticles are bound to a substrate loosely. For example, proteins and DNAs are usually bound to mica by charges. In contact mode, the image is not stable as the molecules move with probe during scan. Tapping mode is well adopted for general imaging because it in general induces less sample damage and tip wear, and generates sharper images than contact mode. However, tapping mode is slower than contact mode if the same scanner is used. In principle, it is the cantilever oscillation amplitude used to control the movement in Z direction in tapping mode. Scanning across a recessed feature, such as a hole, it takes time in the scale of milliseconds for the cantilever oscillation amplitude to increase. Therefore, the cantilever dynamics is the bottleneck in tapping mode. No matter how fast the scanner is, 1–2 Hz is usually used in tapping mode for rough samples. In contrast, the deflection in contact mode changes about 1000 times faster than amplitude in tapping mode. The bottleneck is the scanning mechanism rather than the cantilever itself. For samples with large feature heights, such as cells, contact mode is preferred as it can scan faster over a large area.

Different cantilevers have different resonance frequency. For each cantilever mounted into the instrument, its resonance frequency is usually determined by sweeping frequency and searching the maximum oscillation amplitude, which is

done by a function called “auto tune” in software. The viscoelasticity and density of the medium surrounding the cantilever affect its resonance significantly. In aqueous solution, the resonance frequency drops significantly compared with that in air. For example, the resonance frequency in air of a commonly used silicon nitride cantilever is around 50KHz, while it is about 15KHz in water. In air, the response curve in “auto tune” shows a symmetric Gaussian profile and software can detect its resonance frequency automatically. The same cantilever may show a forest of peaks in aqueous solution. Traditionally, AFM users follow the guideline in the AFM manual to choose a suitable frequency. However, with more and more probes are designed for different applications, it may not be easy to find a recommended frequency in manuals or references for new probes. In today’s AFM, thermal tune is usually equipped to determine the cantilever spring constant. The details of thermal tune will be discussed in the force measurement section. For the sake of easy reading, its principle is briefed here. The thermal noise of the cantilever is measured with PSPD after the tapping piezo is stopped. The power spectra density is calculated for different frequency. Then the resonance frequency is clearly identified, as shown in Fig. 1.7.

The cantilever oscillation amplitude affects the imaging stability and resolution. Larger oscillation amplitude is preferred for rough surface, and smaller amplitude is preferred for high resolution. To make the data consistent and comparable among different AFM instruments, it is desirable to use the same oscillation amplitude, at least comparable if not the same. In practical operation, the amplitude measured by PSPD and lock-in amplifier is a voltage. Different AFM may have different gain in PSPD amplifier and different optical path in the optical lever detection scheme. Therefore, the same voltage output from the lock-in amplifier may measure differ-

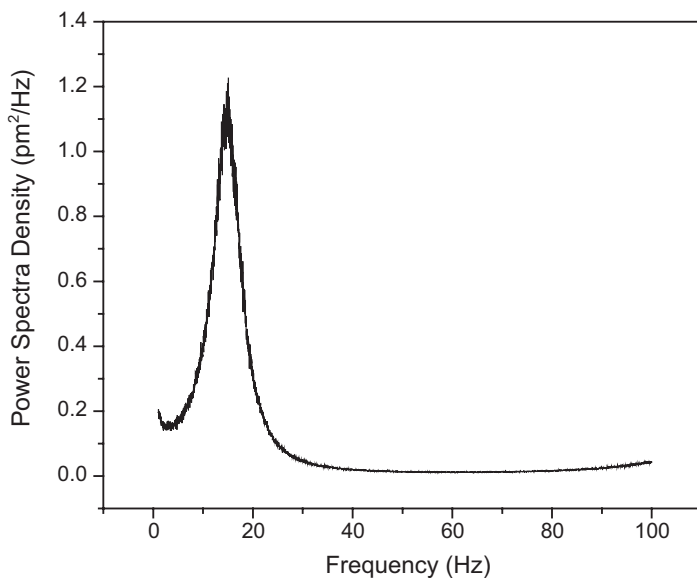


Fig. 1.7 Power spectra density of a silicon nitride cantilever measured in water. The resonance frequency in water is 15 kHz while it is 57 kHz in air

ent oscillation amplitude. Then the scaling factor between voltage and amplitude in nm, also called amplitude sensitivity, must be determined for each type of probe. Here a simple method is described to determine the amplitude sensitivity, the same method can also tell whether the frequency chosen is suitable for tapping mode imaging in aqueous solution. Similar to the force-distance curve in contact mode, the cantilever in tapping mode is ramped by the Z scanner while XY position is fixed. The oscillation amplitude is recorded against the Z position, as shown in Fig. 1.8. When the probe is far from the sample surface, the amplitude does not change significantly with Z position. The slight decrease is caused by the damping effect from the surrounding medium. The narrower the gap between the cantilever and sample surface, the stronger the damping. Once the probe touches the surface at the bottom-most point of each oscillation cycle (shown as mark A in Fig. 1.8), the amplitude starts to decrease rapidly as it is pushed against the surface further. Mark B is the position where the probe fully contacts the sample surface. The slope between A and B is used to measure amplitude sensitivity in nm/V. The steeper the slope, the better the cantilever for imaging as steeper slope means oscillation amplitude is more sensitive to height changes in sample surface. When there are more than one peaks in the tuning curve, the one with steepest slope should be chosen for tapping mode imaging. The amplitude dropping 20% from the corner A is usually a good setpoint.

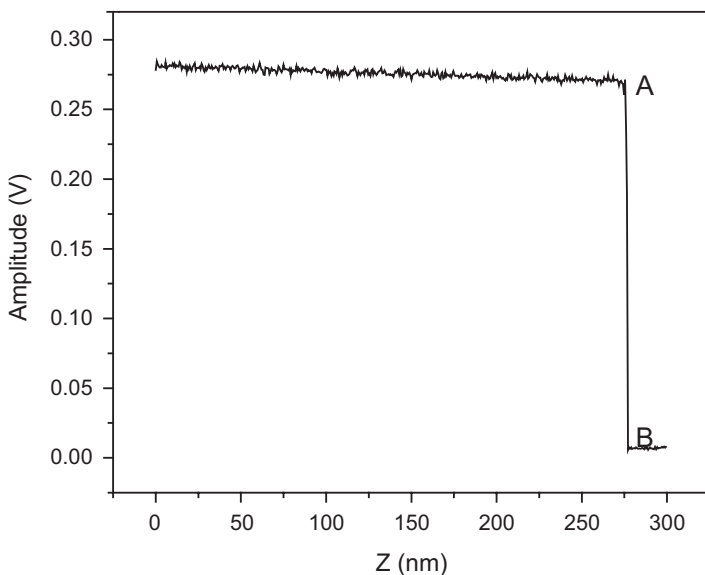


Fig. 1.8 Cantilever oscillation amplitude changes with the Z position in ramp mode. Point A marks the cantilever starts to touch the sample surface at the bottom-most point in each oscillation cycle. Before that, the oscillation amplitude does not decrease significantly. After that, the amplitude decreases rapidly with further decrease in probe-sample distance, until the probe fully contacts the surface, marked as B in the figure. The slope from A to B is used to determine the amplitude sensitivity

Regarding the optimization of feedback loop gains, the tapping mode is similar to contact mode. As discussed earlier, cantilever deflection changes much faster than oscillation amplitude. Contact mode can tolerate higher gains than tapping mode. For example, the gains high enough to cause oscillation in tapping mode may not cause any deleterious effect in contact mode. Optimization of gains is more critical in tapping mode. The oscillation in feedback loop caused by high gains results in noisy images or artifacts. If the gains are too low, the probe will not track the surface properly, resulting in artifacts in images, increased tip wear and sample damage. Therefore, experimental parameters must be tuned more carefully in tapping mode. Among all the parameters, proportional gain, integral gain, setpoint and scan rate are the top parameters to be taken care in tapping mode.

4 PID Feedback Loop

Due to its simplicity and robustness, proportional–integral–derivative controllers (PID controllers) are well adopted in AFM feedback loops, including XY linearization close loop and feedback loop used for topographic imaging. The principle of PID controller and tuning procedure can be found in many text books on process control [11] and articles [12]. Here, we just discuss briefly about its working principle and the tuning procedure suitable for AFM. The schematic diagram of a PID feedback loop is shown in Fig. 1.9.

When the interaction between the tip and sample changes, the output from the optical lever detection system will deviate from the setpoint. The difference $E(t)$ is called error signal. It is logical that the adjustment in Z voltage, ΔV_z , should be proportional to $E(t)$, i.e. $\Delta V_z = PE(t)$. If the proportional gain P is set too low, the response of the system is slow also, and the tip cannot track the sample surface with

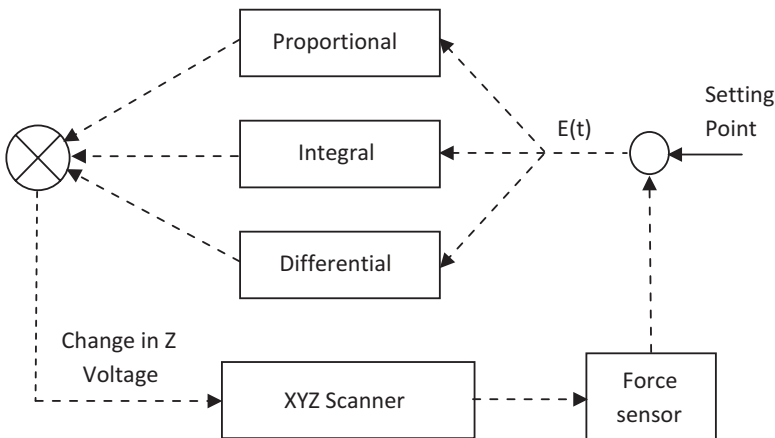


Fig. 1.9 Schematic diagram of PID feedback loop, $E(t)$ is the error signal

a constant probe-sample interaction. If P is set too high, the system will oscillate. The system with a proportional gain only is not sensitive to small error signals. Even the error is small, its integration over time might be large if the error has the same sign. For example, small steady error caused by smooth but slightly slant surface has the same sign. In this case, the integration of error is used to eliminate the steady error. For some small but sharp features, error signal is small but changes rapidly. The proportional and integral components are insensitive to this kind of error. This kind of error can be reduced if the derivative of the error signal is included the feedback loop. Synthesizing the three components, PID feedback loop can be expressed as

$$\Delta V_z = PE(t) + I \int_t^0 E(t) dt + D \frac{dE(t)}{dt} \quad (1.2)$$

In order to obtain good AFM images and extend the tip's life time, the PID parameters must be optimized. The universal method for generic PID feedback loop will not be discussed in this chapter. The tuning procedure described in this chapter is adapted for AFM imaging.

1. Set the scan size to a few μm , say 1–2 μm , even the final scan size is tens of μm .
2. Increase the integral gain until slight oscillation or noise appears in the trace/retrace profiles. The oscillation or noise can usually be eliminated by increase the proportional gains gradually. If it cannot be eliminated, integral gain should be decreased until oscillation/noise disappears.
3. Check the trace/retrace profile, if the probe cannot track the falling slope while the rising slope is tracked properly, reduce the setpoint in tapping mode (or increase the setpoint in contact mode) gradually to improve the tracking.
4. Reduce scan rate if the probe tracking cannot be improved further by reducing setpoint. It should be noted that reducing scan rate must be taken as the last choice because drift and environmental interference might be pronounced during the long imaging time, resulting in distorted images.
5. Increase the scan size to the desired size. If the tracking becomes poor, repeat step 2 to 4 until the image quality is acceptable.

To improve the resolution, sharper probe and less tapping force are always preferred. Less tapping force is usually achieved by smaller cantilever oscillation amplitude. Therefore, 1/3 of normal tapping amplitude is usually used in molecular imaging, e.g. DNA, protein, polysaccharide and other biomolecules. Fig. 1.10 shows a DNA image obtained in tapping mode.

5 Force Mode

In force mode, the AFM probe is ramped up/down by retracting/extending the Z scanner and the cantilever deflection is recorded against Z position, forming a force-distance curve. A typical force-distance curve measured on mica is shown in

Fig. 1.10 DNA image obtained by tapping mode in buffer solution. The image size is $2\ \mu\text{m}$. The DNA height measured from the image is more than $2\ \text{nm}$, showing the interaction force between probe and sample is lower than 300pN , otherwise the height is in general less than $2\ \text{nm}$

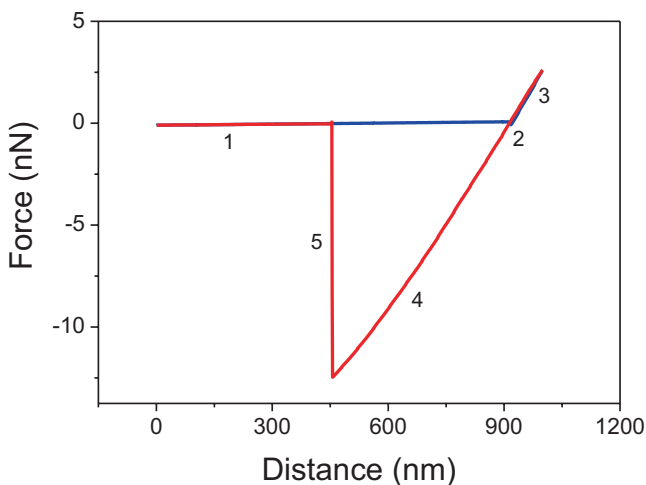
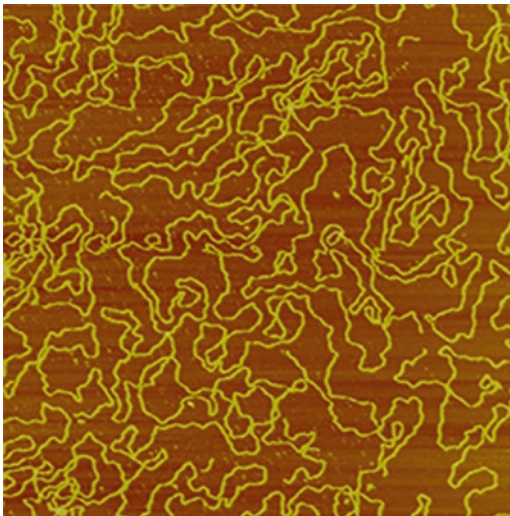


Fig. 1.11 Force-distance curve measured on mica in ambient environment with a relative humidity of 80%. The probe used is a silicon nitride probe (DNP, Bruker)

Fig. 1.11. Before the tip contacts the sample surface, the deflection is a constant, shown as a flat baseline in the force-distance curve, i.e. the segment 1. When the probe is close enough to the sample surface, the attractive force gradient may be greater than the spring constant of the cantilever, snap in will happen, denoted as 2 in the graph. After the probe contacts the surface, the cantilever will bend up with further push against the surface, shown in segment 3. When the preset force is reached, the cantilever will retract from the surface, and deflection decreases accordingly, shown as segment 4. The adhesion force between the probe and sample will

pull the cantilever down further till the force generated by the cantilever is equal to the maximum adhesion force, then the cantilever jumps off from the surface, shown as segment 5, which is usually used to measure the adhesion force. The adhesion force is often used to determine the binding force between antigen and antibody, study surface hydrophobicity by measuring capillary force, and conduct molecular recognition. In ambient environment, capillary force dominates the overall adhesion force. The magnitude of capillary force is determined by the relative humidity and surface hydrophobicity [13]. If the probe and sample are put into controlled environment, interaction mechanism, e.g. the types of interaction force and how the environment changes the interactions, can also be studied. In segment 3, the sample undergoes deformation as well as the cantilever bends up. By studying the relationship between sample deformation and force, material stiffness and modulus can be obtained. If sample undergoes significant plastic deformation, segment 3 and 4 will separate. To obtain modulus under that situation, segment 4 instead 3 will be used to eliminate the effect of plastic deformation. The area enclosed by the different segments is the energy dissipated during each ramp cycle. Material mechanical properties, e.g. Young's modulus, adhesion force, energy dissipation can be extracted from the force-distance curve. In force mode, XY scan is stopped and no lateral force is applied on the sample surface. Scratching on sample surface is rarely observed, unlike contact mode, where the lateral force exists always. In today's AFM, ramps can be programmed at user defined positions or in an array, which are usually implemented by "point and shoot" or "force volume". A series of force-distance curves can be used to construct the topography at a specific force. This method is usually used to image very soft or sticky samples, which are difficult for contact mode and tapping mode.

Comparing force distance curves shown in Figs. 1.6 and 1.11, extension curve and retraction curve are separated in Fig. 1.6. This is because mica is much harder than live cells and the deformation of mica is negligible while live cell undergoes significant plastic deformation. Another obvious difference is the adhesion force, as shown in segment 5 in Fig. 1.11. Mica is hydrophilic and capillary force is strong when measured in ambient environment. In case of live cells, nonspecific binding dominates the overall adhesion force with absence of capillary force. The nonspecific binding force is much smaller than the adhesion force caused by capillary in ambient environment.

Accuracy in force measurement is important for analyzing the interaction mechanism. To obtain accurate force, two parameters need to be calibrated, i.e. cantilever deflection sensitivity and spring constant. Deflection sensitivity measures how many nm in cantilever deflection correspond to 1 V in the PSPD output. It is measured by ramping the probe on a hard surface, for example sapphire. The deformation of such surface is negligible. So the displacement of Z scanner is the same as the deflection of the cantilever, i.e. the slope of the segment 3 in Fig. 1.11 should be 1. In force-distance curve, deflection sensitivity is determined by fitting the segment 3 to a straight line to obtain the slope. The deflection sensitivity making the slope to be 1 is the calibrated value. This process has been automated in today's AFM. To get accurate and repeatable value, the snap-in point and the approach/retract turning

point are usually excluded from the calculation. Deflection sensitivity is determined by the cantilever length and the sensitivity of PSPD. Short cantilever produces better sensitivity and is preferred in measuring displacement in pm range. For a given AFM, the cantilevers with the same length should have the same deflection sensitivity. In real operation, the laser spot may not be aligned to the same position on the cantilever every time. It is normal that the deflection sensitivity of the same cantilever varies slightly after realigning the laser. This is because the change in laser spot position affects the effective length of the cantilever. It is a good practice to measure the deflection sensitivity each time after the laser is re-aligned. With the calibrated deflection sensitivity, how many nm the cantilever deflects can be calculated from the deflection in voltage.

For a cantilever with rectangular cross section, its spring constant can be expressed as

$$k = \frac{Et^3w}{4L^3} \quad (1.3)$$

where E is the Young's modulus of the cantilever material, e.g. silicon or silicon nitride,

t , w , and L are the thickness, width, and length of the cantilever respectively.

The width and length of a cantilever can be controlled precisely through micro fabrication technology, while the thickness bears more deviation due to its manufacturing process. 10% thickness error will result in about 30% error in spring constant. The nominal spring constant on probe boxes can only be used as an indicative value. Each cantilever must be calibrated to get correct force value. Several methods have been developed to measure cantilever spring constant. The simplest way is to measure the resonance frequency f and check the probe factor b from reference book. The spring constant is calculated by

$$k = b * f^3 \quad (1.4)$$

This method is very easy to use as the resonance frequency can be obtained by "auto tune" in tapping mode. The major drawback is its poor accuracy because the dimensions may be slightly different from those in the reference. For example, the cantilever width affects its spring constant, but not its resonance frequency. If the actual width of cantilever is different from that in the reference, the calculated spring constant will deviate from the real value.

To improve this situation, top view geometry (length and width) is added into the equation as [14].

$$k = 2\pi^3 \sqrt{\frac{\rho^3}{E}} L^3 w f^3 \quad (1.5)$$

where ρ and E are the density and Young's modulus of cantilever material,

L and w are the length and width respectively, usually measured through a well calibrated micrograph of scanning electron microscopy or optical microscopy.

A more accurate method was developed in reference [14] by adding a known mass and measuring the resonance frequency shift, i.e.

$$k = (2\pi)^2 \frac{M}{\left(\frac{1}{f_i}\right)^2 - \left(\frac{1}{f_0}\right)^2} \quad (1.6)$$

where M is the mass added to the cantilever free end, f_0 and f_i are resonance frequencies before and after the mass is added respectively.

This method involves gluing a particle with known mass to the end of cantilever. It is not trivial even with a detailed protocol available [15, 16]. Furthermore, it is even more troublesome to remove the particle after the spring constant is calibrated. Therefore, force measurements are usually done before the calibration. After all experiments are finished, the calibration is carried out and the measurement results are rescaled with the correct spring constant. This method is complicating and the cantilever cannot be used after calibration. This method is rarely used in biological application despite its accuracy.

All the above discussed methods do not measure cantilever *in-situ*. In practice, the laser may not be aligned to the same position as in spring constant measurement. The difference in laser alignment results in difference in cantilever effective length. With the advances in AFM instrumentation, the thermal noise of cantilever has been used to calculate its spring constant. After the deflection sensitivity is calibrated, the cantilever is lifted from the sample surface by at least 100 μm and the random motion of cantilever free end is recorded for a period of time. 10 seconds are usually enough to get accurate results. The power spectral density (PSD) is then calculated by Fourier Transformation over the noise recorded, as shown in Fig. 1.7. According to Equipartition Theorem [17],

$$\frac{1}{2} m \omega_0^2 z^2 = \frac{1}{2} k_B T \quad (1.7)$$

where m is the effective mass of the cantilever,

ω_0 and z are the angular frequency and noise amplitude of cantilever free end respectively,

k_B and T are Boltzman constant = 1.3805×10^{-23} joules/Kelvin and absolute temperature in Kelvin,

$\langle \rangle$ means averaging over time, which is obtained by integrating PSD over frequency.

Considering $\frac{1}{2} k z^2 = \frac{1}{2} k_B T$, the cantilever spring constant k can be obtained

$$k = k_B T / z^2 \quad (1.8)$$

The mean square of free end amplitude $\langle z^2 \rangle$ is the area under the peak of power spectra density profile.

This method is well accepted because it neither relies on the cantilever geometry, as in method 1 and 2, nor demands the complicating procedure, as in the mass adding method. After further improvement by Butt and Jaschke [18] followed by Hutter [19], the accuracy achieved by the thermal noise method is reliable [20]. In most of today's AFM, this method is automated in software. The frequency range covers from a few KHz to 2 MHz. Virtually all the commercial available cantilevers can be calibrated with this method. For some ultra soft cantilevers, the resonance frequency in liquid is below 2KHz. The Z scanner noise and laser pointing noise in some AFM may limit the accuracy in spring constant measurement. In such case, the spring constant measured in air is a good estimation.

Determining Young's modulus through force-distance curve has been extensively studied [21]. Hertz, DMT, JKR and Maugis models are commonly used to measure Young's modulus of materials [22]. In all the models, good understanding of the probe shape and size is as important as accurate measurement of force. For sample deformation in a few nm, the AFM tip is usually modeled as a sphere. For polymer samples, a few nm deformation produces enough force for accurate measurement in AFM. DMT model with spherical probe is usually used [2].

$$F = \frac{4}{3} E^* \sqrt{R} d^{3/2} + F_{ad} \quad (1.9)$$

where F is the force measured by the probe,

F_{ad} is the adhesion force between tip and sample,

R is the radius of the tip,

d is the sample deformation,

E^* is the reduced Young's modulus $= \frac{E}{1-\nu^2}$, ν is the Poisson Ratio of the material. Young's modulus of the probe material is usually much higher than that of the sample. The deformation of probe is negligible.

Tip geometry can be obtained by either high resolution electron microscopy or tip deconvolution. In the latter method, a reference sample with sharp features is scanned and the morphological dilation is analyzed to extract the tip geometry [23]. It may cause tip wear to scan over such reference sample as it is rough and very hard. So the scan parameters must be optimized carefully. As the relationship between E^* and \sqrt{R} is linear, \sqrt{R} can also be calibrated after sample measurements and rescale E^* with calibrated \sqrt{R} .

For soft materials, such as live cells, the deformation is usually in the range of tens of nm, a conical shape is a good estimation of tip shape. In liquid, adhesion force is negligible, Hertz mode with conical tip shape is usually used for live cell measurement,

$$F = \frac{2}{\pi} E^* (\tan \alpha) d^2 \quad (1.10)$$

where F is the force measured by the probe,

E^* is the reduced Young's modulus of the material,

d is the sample deformation,

α is the half angle of the conical probe.

In practical operation, probes with pyramidal shape are usually used, where the half angles in the two directions are α and β respectively. Equation (1.10) should be revised accordingly,

$$F = \frac{4}{\pi\sqrt{\pi}} E^* \sqrt{\tan \alpha \cdot \tan \beta} d^2 \quad (1.11)$$

In AFM measurement, the force is recorded against the scanner Z position rather than the sample deformation. When the cantilever is pushed against the sample, the cantilever bends up while the sample deforms. The sample deformation can be calculated as follow,

$$d = (z - z_c) - (def - def_0) \quad (1.12)$$

where z_c is the scanner position at the contact point,

def_0 is the baseline of cantilever deflection,

z and def are the scanner position and cantilever deflection in the force-distance curve.

Baseline deflection def_0 can be obtained easily from force-distance curve. Contact point z_c for hard materials can be obtained by the intersection of the baseline and linear slope. For soft materials, such as cells, it is not easy to tell accurately where the probe starts to contact the sample, as shown in Fig. 1.6. It is a good practice to keep both E^* and z_c as two unknown parameters to be extracted through fitting the force-distance curve to a suitable model. During the fitting procedure, all others quantities are measured from force-distance curve. The reduced Young's modulus extracted from the force curve shown in Fig. 1.6 is 50 KPa. In this fitting, Hertz model with conical tip shape is adopted. The half angles of pyramidal tip are 20° and 17.5° , and spring constant is 0.01 N/m.

Soft cantilever is preferred for force measurement [24]. Deformation is measured by subtracting cantilever deflection from the scanner movement in Z. For soft cantilever, the cantilever deflection and scanner movement in Z is usually much larger than sample deformation. Therefore, soft cantilevers usually produce more error in deformation measurement. On the other hand, force measurement may less accurate if too stiff cantilever is used. Both situations can lead to less accurate Young's modulus. Therefore, it is important to choose a proper cantilever spring constant for a specific modulus range. As a rule of thumb, the ratio of sample deformation to cantilever deflection between 0.1 and 0.2 is a good start to try. In real measurement, the error in deflection sensitivity contributes a significant part in total error as it affects the accuracy in both force and deformation. It must be calibrated carefully. During the deflection sensitivity calibration, at least 5 measurements are

needed to calculate the average. In model selection, a rule of thumb is that DMT model with spherical tip shape is used for the scenario with deformation less than the radius of the tip and Hertz model with conical tip shape is used for large deformation in tens of nm. The Poisson Ratio is usually unknown for most of materials, especially biomaterials. 0.5 is usually used in live cell measurement.

Adhesion force between AFM tip and sample is obtained directly from force-distance curves. There might be a few binding events existing between the AFM tip and substrate. The last force step (jumping off) can be considered as single unbinding [13]. There is a slim chance that two or more unbinding events happen at the last force step simultaneously. To rule out multi-unbinding event, multiple force-distance curves are recorded, and the last force steps are extracted and plotted in a histogram. By reading the peak position in histogram, the most likelihood rupture force of single binding is obtained. Using functionalized probe, adhesion force has been used in measuring hydrophobicity, function group/molecule recognition, and antigen-antibody binding force study.

Another application of force-distance curve is to stretch single molecules, including proteins, polysaccharides and DNAs. By stretching, a protein molecule is unfolded mechanically. This kind of measurements are pursued for a variety of reasons, including fundamental questions about folding, structure and how protein sequence contributes to that. Protein structures are traditionally determined by X-ray crystallography. However, it might not be practical to perform this technique on membrane proteins. Force curve is one of the few ways to gain insight into the protein structure. Fig. 1.12 is a typical unfolding curve of titin, which is an 8-mer construct of IG27 domain. The saw teeth in the retraction curve are caused by unfolding of the domains. When the stretching force reaches the critical value (marked as A in the figure), one domain is unfolded and force decreases suddenly. After the domain is unfolded (marked as B), the force increases gradually as the cantilever stretches the molecule further. The second domain starts to unfold upon the critical force reached (marked as C).

By the fitting the domain extension curve (e.g. from B to C) to worm like chain model [25],

$$F = \frac{kT}{p} \left[\frac{1}{4} \left(1 - \frac{x}{L_c} \right)^{-2} - \frac{1}{4} + \frac{x}{L_c} \right] \quad (1.13)$$

the persistence length p and contour length L_c are obtained. In the fitting, the molecular length x is determined by subtracting cantilever deflection from Z scanner traveling distance, similar to the deformation calculation in indentation experiment.

To perform the stretching experiment, one end of the molecule is tethered to a gold substrate by thiol group. The other end is picked up by a soft probe with spring constant ranging from 0.01 N/m to 0.1 N/m. The probe may pick up many molecules if the concentration is too high. On the other hand, many trial and errors have to be performed to pick up a molecule in case that the concentration is too low. 50 μ g/ml is a good start concentration of titin. Take 25–50 μ L of the titin solution

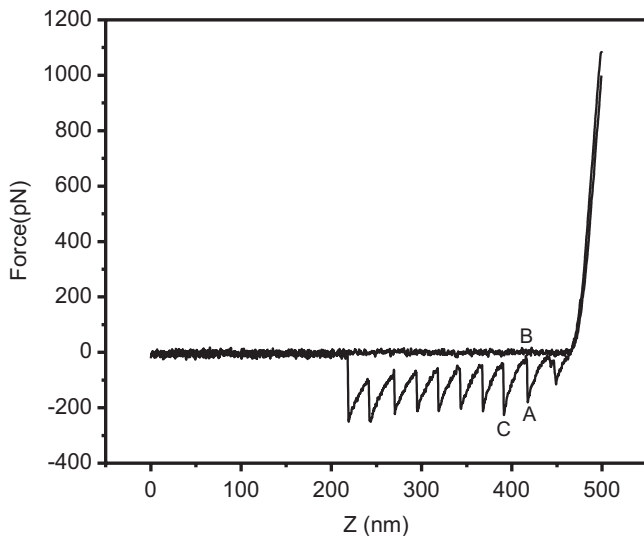


Fig. 1.12 Typical pulling curve of titin unfolding (8-mer construct of IG27 domain). Each saw tooth corresponds to an unfolding event. The probe is retracted after staying on the surface for a fraction of second to catch a protein molecule. During retraction, the adhesion force pulls the cantilever down until reaching critical force at A, where one domain starts to unfold. The force is released because the molecular length increases suddenly. At point B, the domain is fully unfolded. The force increases as the cantilever stretches the molecule further. With the continuing pulling, another critical force is reached at point C, where a new domain starts to unfold

and drop onto a fresh gold surface. After incubation at room temperature for 15 minutes, rinse it with 1–2 mL PBS buffer. Then the sample is mounted into an AFM to perform the force measurement. If the chance of picking up is too low, keeping the probe staying longer on the surface will increase the chance significantly. The stay can be extended to seconds.

6 Peak Force Tapping

AFM was applied to study biological materials from its very start [26]. However, the adoption of this technique in biological and biomedical applications is slow even it is compatible with biological environments. This is mainly because the information provided by AFM is lack of biological specificity. The recent developments in AFM are mainly in expanding its functionalities. Force mode can provide biological specific information by extracting a variety of mechanical properties from force-distance curve, which is typically measured at 1 curve/second. It is prohibitive to achieve the typical spatial resolution of tapping mode due to the intensive time consumption in traditional force mode.

To speed up the force mapping, pulse force mode was introduced in 1997 [27]. In this mode, the probe is modulated by fast sinusoidal ramping rather than the linear ramping in traditional force mode. Pulse force mode improves the efficiency by 3 orders. However, the poor force control in this mode limits its usage in high resolution applications where the probe-sample interaction force should be in the range of sub-nN to several nNs. In force measurement, the cantilever deflection may change with ramping even there is no change in probe-sample interaction because,

1. The ramping motion may not be in parallel with the laser optical axis. Thus, the laser spot on cantilever moves with ramping, resulting in non-flat baseline. In addition, the ramping motion may not follow a straight line. This leads to a non-linear baseline.
2. When it jumps off from the sample surface in pulling, the cantilever often oscillates at its resonance frequency. The oscillation is severe for soft cantilevers. In ambient environment, the capillary force increases the total adhesion, making the oscillation more pronounced. The oscillation may not be fully damped at the start of the next ramp and it will affect the measurement results.
3. The viscosity of media (liquid or air) can cause deflection change during ramping. This effect becomes severe when the cantilever is close to the sample surface. The damping from the media trapped between the cantilever and sample surface becomes stronger with the decrease in gap.

With the increase in ramping speed, effects of all these factors become even severe. These parasitic deflections contaminate force-distance curves, making accurate force control difficult, especially at high speed. To overcome this issue, Su et al. implemented a method to characterize and parameterize the parasitic deflections for each instrument [28]. After parasitic deflections are removed, clean force-distance curve can be obtained at the speed of KHz by modulating the Z scanner with sinusoidal wave. Within a modulation cycle, the repulsive force reaches its maximum at the bottom-most point, similar to traditional force mode. The peak force (maximum force) is used to control Z scanner movement to make the probe track the sample surface. Compared with traditional force mapping, the peak force tapping mode is more accurate in force measurement (tens of pN can be achieved), and ramping speed is at least 3 orders faster. It is worth noting that the ramping rate is still far below the cantilever resonance frequency, which is typically from tens of KHz to hundreds of KHz. The cantilever works in quasi-static mode. This peak force tapping mode has been implemented in commercial AFM [29], known as ScanAsyst and PeakForce QNM.

Peak force tapping mode does not rely on cantilever dynamics, making it not necessary to search the cantilever resonance frequency. Its operation is also independent of environment. In tapping mode, the cantilever resonance frequency depends on its surrounding media (liquid or air), temperature and as well as cantilever itself. Therefore, the cantilever must be tuned under the same environment as the real experiments. On contrast, no matter which cantilever, no matter in liquid or air, the operation is the same for peak force tapping mode. As discussed early in this chapter, the cantilever deflection drift due to environmental influence, especially

temperature, prohibits the deflection setpoint being set very close to that of free cantilever, making imaging at pN a challenging job. In peak force tapping mode, cantilever deflection drift is corrected at each ramping cycle, so cantilever deflection drift is not an issue anymore. Beside superior force control, another achievement in peak force tapping is that operation parameters are automatically optimized by software. In peak force tapping mode, the Z scanner is moved up/down to maintain a constant peak force. As the error in peak force is linear to topographic error and PID controller is also a linear controller, it is easy to implement automatic parameter optimization. While in tapping mode, the relationship between amplitude and probe-sample distance has hysteresis, i.e. the extension curve and retraction curve do not overlap. This makes it difficult to implement automatic parameter optimization even the amplitude linearly responds to the distance during approach curve, as shown in Fig. 1.8. With superior force control in the range of tens pN, the integrity of biomolecules and probe sharpness are well maintained during the scan. Sub molecular resolution can be readily achieved. DNA double helix structure has been measured with peak force tapping [30].

With a calibrated deflection sensitivity, force-deformation curve is reconstructed by subtracting deflection from the scanner Z movement, as done in traditional force mode. From each curve, Young's modulus, adhesion force, deformation, energy dissipation, and peak force in each tapping cycle are extracted. These material mechanical properties are mapped into different channels and form images for spatial distribution analysis. With the knowledge of tip geometry, the deformation data can be easily converted to indentation hardness [31]. Compared with traditional force mode, the peak force tapping is thousands of times faster as well as providing better force control, making it an ideal mode for high resolution topographic and mechanical imaging. It has been used to image sub-molecular structure of protein molecules [32].

7 Molecular Recognition

Recognizing molecules on substrates or cell membrane based on specific binding has attracted interest from many researchers since more than a decade ago. Force mapping is a commonly used approach to identify molecules and study the ligand-receptor interaction under different environments [33–35]. As discussed previously, force mapping is in general slow and lack of spatial resolution. To improve the speed, a dynamic recognition microscopy was developed [36], where a functionalized probe is oscillated with an amplitude smaller than the length of linker molecule (the typical length is about 6 nm). When recognition happens, the oscillation amplitude of cantilever is decreased due to the interaction force. During the operation, the binding is not disassociated by the cantilever oscillation. The binding pair is ruptured by the lateral pulling force during scan when the distance between the molecule and tip reaches the linker length. Therefore, the size of recognized molecules is dilated by two times of the linker length. With this progress, molecular

recognition can be done at the speed of normal AFM imaging. However, this method cannot provide quantitative binding force.

Another technical challenge is the surface chemistry to functionalize the probe and the substrate. The procedure for probe functionalization includes linkage design and covalently coupling the ligand to the tip surface. The bonding between the ligand and tip surface should be significantly stronger than the ligand - receptor bonds. Otherwise, the functionalized probe may lose its ligand to the substrate, and lose the recognition capability. Poly(ethylene glycol) (PEG) is a well adopted linker because it is water soluble and non-toxic [37]. PEG has been used in a wide range of applications in surface modification and clinical research. The detailed protocols are described in many articles on force measurement, e.g. references [33–37]. To illustrate the concept, the procedure is described here briefly. The first step is to clean the probe thoroughly. This is typically implemented by incubating AFM probe in piranha solution ($\text{H}_2\text{SO}_4/\text{H}_2\text{O}_2$, 90/10 (v/v)) for 30 mins and then rinsing with deionized water. After dried by N_2 blow, the probe is subjected to water plasma to generate SiOH groups on the probe surface [38]. The second step is to bind amines to the tip surface by an esterification protocol described in reference [33]. The third step is to conjugate the linker to the amines on the tip surface. The engineered PEG linker has N-hydroxysuccinimidyl (NHS) residue on one end and a function group to connect the ligand on the other end. The NHS group is used to bind the linker to the amines. The fourth step is to link the ligand to the function group on the end of the engineered linker. PDP (2-pyridyldithiopropionyl residue) and NTA (Ni-Nitriloacetate) [39] are commonly used function groups.

On the substrate side, different surface-binding strategies should be adopted for the different properties of biological samples. Some receptor proteins strongly adhere to mica surface through hydrophobic or electrostatic forces. In this case, direct adsorption provides sufficiently strong anchoring for recognition experiments. Another option is to use sulfur-gold chemistry. Atomically flat gold surface is prepared as a substrate, as in titin pulling experiment discussed previously. If silicon or mica is used as substrate for water-soluble receptors, the same surface chemistry as in probe functionalization can be used. For receptors on cells, directly growing the cells on substrate is typically used. To enhance the cell adhesion to the substrate, the methods discussed in live cell imaging section can also be used in molecular recognition.

Since peak force tapping measures adhesion force directly. With properly functionalized probes, it can be used to recognize molecules or function groups [40]. In addition to molecules on substrate, Fig. 1.13 shows molecular recognition on cell membrane. In this example, red blood cells develop knobs on their surface after infected with malaria parasites. The probe is functionalized with PEG linker and CD36, which is used to recognize Plasmodium falciparum erythrocyte membrane protein 1 (PfEMP1) [41]. It is worth noting that the CD-36 binding sites locate solely on the knobs. Another interesting finding is that the adhesion is free of any topographic artifact, as the debris (marked by white arrow) does not show adhesion force while it is clearly shown in topography. This makes the binding force mapping clean and quantitative.

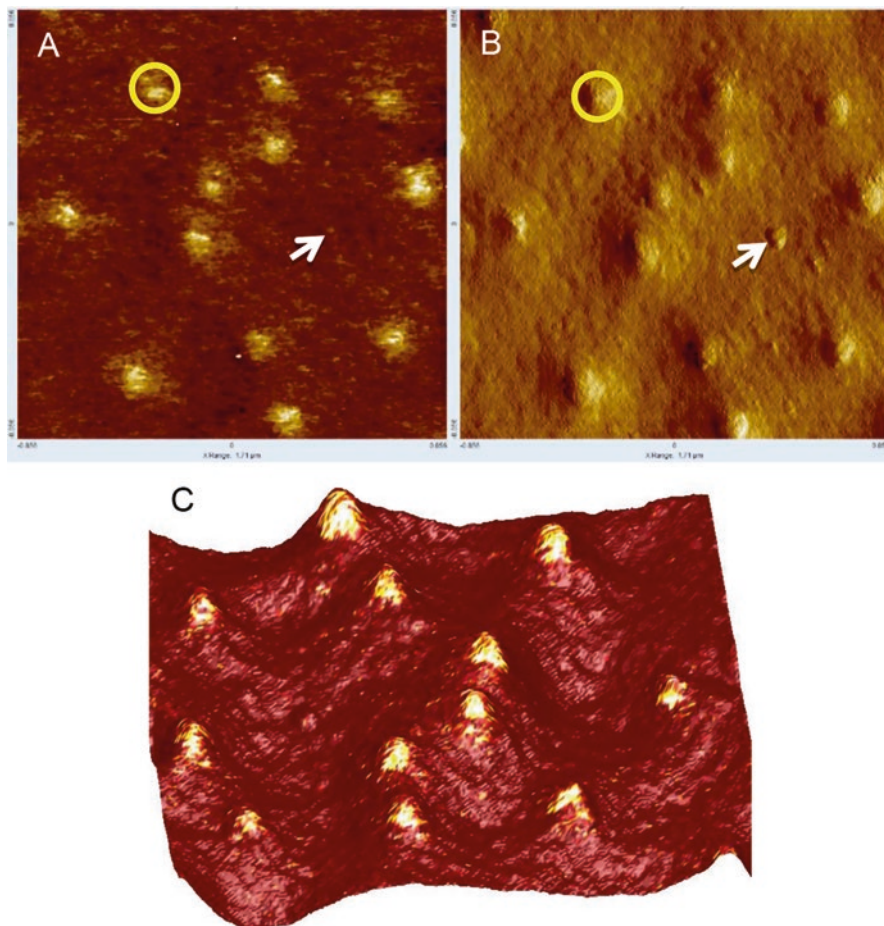
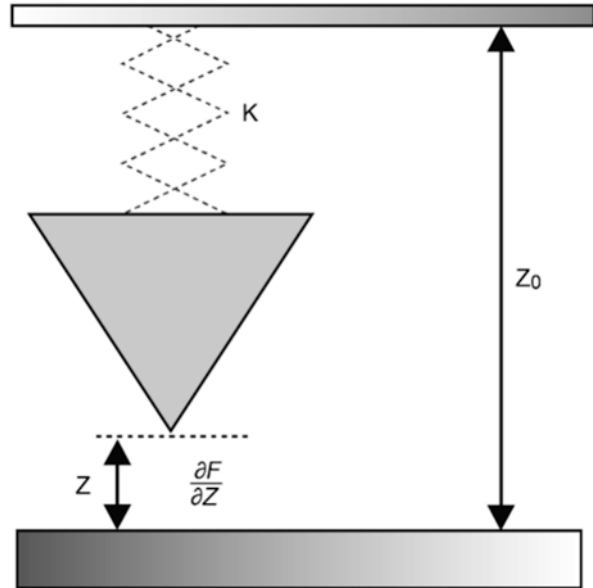


Fig. 1.13 CD-36 binding site recognition on malaria infected red blood cells by peak force tapping mode. (a) and (b) are adhesion force and peak force error images respectively. Peak force error image reveals the detailed topographic information. (c) is the overlay of adhesion force over peak force error. CD-36 binding sites have one-to-one correspondence with knobs, as shown by the circled area in (a) and (b). The debris marked by arrow in (b) does not show adhesion force in A, proving that there is no cross talk between topography and adhesion force. The adhesion force image is topographic artifacts free. (Image courtesy of A. Li, National University of Singapore)

8 Frequency Modulation Mode

Unlike tapping mode where amplitude is used as feedback signal, frequency modulation uses a frequency shift as the feedback signal. It was first introduced by Albrecht T. et al. in 1991 [42]. In this mode, the probe oscillates at a frequency close to its resonance. The resonance frequency of the cantilever is affected by the force gradient between tip and sample. This effect is illustrated in Fig. 1.14. When a

Fig. 1.14 The working principle of a frequency modulation AFM. When a cantilever oscillates in a force field, the force gradient will affect the effective spring constant, and then the resonance frequency



cantilever oscillates in a force field, the effective spring constant of the cantilever is changed by the force gradient; leading to the shift in resonance frequency. Mathematically, the effective spring constant is the superposition of the nature spring constant and the local force gradient. During a scan, the changes of surface topography leads to the resonance frequency shift. The feedback loop maintains a constant frequency by vertically moving the scanner at each location. The constant frequency is called frequency setpoint.

Under small amplitude situation, the frequency shift is proportional to the force gradient of the tip-sample interactions. Compared with long-range interactions, the force gradient of short-range interactions is much higher, so the short-range interactions contribute much more than the long-range interactions. This is believed to be the fundamental reason for high resolution imaging. In spite of its potential in high resolution imaging, frequency modulation is not well adopted in commercial AFM because it does not work stably in ambient environment. The main reason is the capillary between probe and sample cause strong adhesion force. Frequency modulation is mainly used in high vacuum environment, where amplitude modulation does not work due to the high quality factor of the cantilever in vacuum.

In summary, working principles of different AFM modes are discussed in this chapter. Based on the understanding of the working principles, users can choose suitable working mode, proper cantilever, and optimize operation parameters during imaging. It also helps identify image artifacts and interpret AFM results.

Reference

1. Binnig G, Quate CF, Gerber C. Atomic force microscope. *Phys Rev Lett*. 1986;56:930–3.
2. Israelachvili JN. Intermolecular and surface forces. London: Academic; 1992.
3. Heaton MG, Prater CB, Kjoller KJ Lateral and chemical force microscopy mapping surface friction and adhesion. Bruker application note AN5, Rev. A1. 2004
4. Fritz J. Cantilever biosensors. *Analyst*. 2008;133:855–63.
5. Thimonier J, Montixi C, Chauvin JP, He HT, Rocca-Serra J, Barbet J. Thy-1 immunolabeled thymocyte microdomains studied with the atomic force microscope and the electron microscope. *Biophys J*. 1997;73:1627–32.
6. Henderson E, Haydon PG, Sakaguchi DS. Actin filament dynamics in living glial cells imaged by atomic force microscopy. *Science*. 1992;257:1944–6.
7. Nagayama S, Morimoto M, Kawabata K, Fujito Y, Ogura S, Abe K, Ushiki T, Ito E. AFM observation of three-dimensional fine structural changes in living neurons. *Bioimages*. 1996;4:111–6.
8. Babcock KL, Prater CB. Phase imaging: beyond topography. Bruker application note AN11, Rev. A1. 2004
9. McLean RS, Sauer BB. Tapping-mode AFM studies using phase detection for resolution of Nanophases in segmented polyurethanes and other block copolymers. *Macromolecules*. 1997;30:8314–7.
10. Lv Z, Wang J, Chen G, Deng L. Imaging recognition events between human IgG and rat anti-human IgG by atomic force microscopy. *Int J Biol Macromol*. 2010;47:661–7.
11. Bennett S. A history of control engineering, 1930–1955. London: IET; 1993.
12. Ang KH, Chong G, Li Y. PID control system analysis, design, and technology. *IEEE Trans Control Syst Technol*. 2005;13:559–76.
13. Sun W, Neuzil P, Kustandi TS, Oh S, Samper VD. The nature of the Gecko Lizard adhesive force. *Biophys J*. 2005;89:L14–7.
14. Cleveland JP, Manne S, Bocek D, Hansma PK. A nondestructive method for determining the spring constant of cantilevers for scanning force microscopy. *Rev Sci Instrum*. 1993;64:403–5.
15. Ducker WA, Senden TJ, Pashley RM. Direct measurement of colloidal forces using an atomic force microscope. *Nature*. 1991;353:239–41.
16. Preuss M, Butt H-J. Direct measurement of particle–bubble interactions in aqueous electrolyte: dependence on surfactant. *Langmuir*. 1998;14:3164–74.
17. Greiner W, Neise L, Stöcker H. Thermodynamics and statistical mechanics. New York: Springer; 2001.
18. Butt H-J, Jaschke M. Calculation of thermal noise in atomic force microscopy. *Nanotechnology*. 1995;6:1–7.
19. Hutter JL. Comment on tilt of atomic force microscope cantilevers: effect on spring constant and adhesion measurements. *Langmuir*. 2005;21:2630–2.
20. Ohler B. Cantilever spring constant calibration using laser Doppler vibrometry. *Rev Sci Instrum*. 2007;78:063701.
21. Oliver WC, Pharr GM. Measurement of hardness and elastic modulus by instrumented indentation: advances in understanding and refinements to methodology. *J Mater Res*. 2004;19:3–20.
22. Cappella B, Dietler G. Force-distance curves by atomic force microscopy. *Surf Sci Rep*. 1999;34:1–104.
23. Belikov S, Erina N, Huang L, Su C, Prater C, Magonov S, Ginzburg V, McIntyre B, Lakrout H, Meyers G. Parametrization of atomic force microscopy tip shape models for quantitative nanomechanical measurements. *J Vac Sci Technol B Microelectron Nanometer Struct Process Meas Phenom*. 2009;27:984–92.
24. Shao Z, Mou J, Czajkowsky DM, Yang J, Yuan J-Y. Biological atomic force microscopy: what is achieved and what is needed. *Adv Phys*. 1996;45:1–86.
25. Bustamante C, Marko JF, Siggia ED, Smith S. Entropic elasticity of lambda-phage DNA. *Science*. 1994;265:1599–600.

26. Butt H-J, Wolff EK, Gould SAC, Dixon Northern B, Peterson CM, Hansma PK. Imaging cells with the atomic force microscope. *J Struct Biol.* 1990;105:54–61.
27. Krottil H-U, Stifter T, Waschipky H, Weishaupt K, Hild S, Marti O. Pulsed force mode: a new method for the investigation of surface properties. *Surf Interface Anal.* 1999;27:336–40.
28. Su C, Lombrozo PM Method and apparatus of high speed property mapping. 2010
29. Pittenger B, Erina N, Su C. Quantitative mechanical property mapping at nanoscale with PeakForce QNM. Bruker application note AN128, Rev. B0. 2012
30. Pyne A, Thompson R, Leung C, Roy D, Hoogenboom BW. Single-molecule reconstruction of oligonucleotide secondary structure by atomic force microscopy. *Small.* 2014;10:3257–61.
31. Swadener JG, George EP, Pharr GM. The correlation of the indentation size effect measured with indenters of various shapes. *J Mech Phys Solids.* 2002;50:681–94.
32. Rico F, Su C, Scheuring S. Mechanical mapping of single membrane proteins at submolecular resolution. *Nano Lett.* 2011;11:3983–6.
33. Hinterdorfer P, Baumgartner W, Gruber HJ, Schilcher K, Schindler H. Detection and localization of individual antibody-antigen recognition events by atomic force microscopy. *Proc Natl Acad Sci U S A.* 1996;93:3477–81.
34. Hinterdorfer P, Schilcher K, Baumgartner W, Gruber HJ, Schindler H. A mechanistic study of the dissociation of individual antibody-antigen pairs by atomic force microscopy. *Nanobiology J Res Nanoscale Living Syst.* 1998;4:39–50.
35. Baumgartner W, Hinterdorfer P, Ness W, Raab A, Vestweber D, Schindler H, Drenckhahn D. Cadherin interaction probed by atomic force microscopy. *Proc Natl Acad Sci.* 2000;97:4005–10.
36. Raab A, Han W, Badt D, Smith-Gill SJ, Lindsay SM, Schindler H, Hinterdorfer P. Antibody recognition imaging by force microscopy. *Nat Biotechnol.* 1999;17:901–5.
37. Hinterdorfer P, Kienberger F, Raab A, Gruber HJ, Baumgartner W, Kada G, Riener C, Wielert-Badt S, Borken C, Schindler H. Poly(Ethylene Glycol): an ideal spacer for molecular recognition force microscopy/spectroscopy. *Single Mol.* 2000;1:99–103.
38. Kiss E, Gölander C-G. Chemical derivatization of muscovite mica surfaces. *Colloids Surf.* 1990;49:335–42.
39. Conti M, Falini G, Samori B. How strong is the coordination bond between a histidine tag and Ni – Nitrioltriacetate? An experiment of Mechanochemistry on single molecules. *Angew Chem.* 2000;112:221–4.
40. Pfreundschuh M, Alsteens D, Hilbert M, Steinmetz MO, Müller DJ. Localizing chemical groups while imaging single native proteins by high-resolution atomic force microscopy. *Nano Lett.* 2014;14:2957–64.
41. Baruch DI, Ma XC, Pasloske B, Howard RJ, Miller LH. CD36 peptides that block cytoadherence define the CD36 binding region for *Plasmodium falciparum*-infected erythrocytes. *Blood.* 1999;94:2121–7.
42. Albrecht TR, Grütter P, Horne D, Rugar D. Frequency modulation detection using high-Q cantilevers for enhanced force microscope sensitivity. *J Appl Phys.* 1991;69:668–73.